PHYSICAL REVIEW B VOLUME 45, NUMBER 21 1 JUNE 1992-I

Spiral-spin-density-wave states in fcc iron: Linear-muffin-tin-orbitals band-structure approach

O. N. Mryasov, V. A. Gubanov, and A. I. Liechtenstein
Institute of Chemistry, Ural Science Center, Academy of Sciences, Sverdlovsk, U.S.S.R.

(Received 19 August 1991; revised manuscript received 3 December 1991)

A method for electronic-structure calculations of noncollinear magnetic structures has been developed based on the linear-muffin-tin-orbitals approach. Calculations of total energies and magnetic moments for various spiral-spin-density-wave states of fcc iron have been carried out. The results obtained show that the ground state of fcc iron is the spiral-spin-density-wave state. With the increase of the number of valence electrons (as in fcc Co) ferromagnetic ordering stabilizes essentially, whereas the decrease of that (as in fcc Mn) results in the antiferromagnetic ordering of spin moments.

I. INTRODUCTION

The magnetic and electronic properties of fcc iron (γ-Fe) have been traditionally the subject of many experimental[1,2] and theoretical[3,4] investigations. This interest is connected both with the intermediate position of γ-Fe among the magnetic 3d metals and the known "Invar" problem. Previous band-structure calculations[3,4] took into account atomic-magnetic-moment-value variations only, and the collinear magnetic structures were considered. However, recent neutron diffraction experiments[2] lead to the conclusion that the ground state of γ-Fe is the spiral-spin-density-wave (SSDW). Hirai[5] investigated magnetic structure of γ-iron basing on the results of unenhanced magnetic susceptibility calculations and reached a similar conclusion. But direct band-structure calculations of such states have not been carried out up to now. In the present paper we develop a direct computational approach based on the linear-muffin-tin-orbitals (LMTO) method,[6] which allows one to describe both continuous changes in magnetic moment value and orientation, i.e., to consider noncollinear magnetic systems with SSDW states. The method suggested is applied for the calculations of magnetic and electronic structure of different spiral-spin-density waves in γ-iron, in the range of wave vector $\mathbf{q}=q(0,0,1)$, $\theta=\pi/2$ between $q=0$ and 1 (in units of $2\pi/a$ where a is the lattice constant). Using the results of these band-structure calculations we have estimated also the parameters of exchange interactions in the scope of the Heisenberg model.[7,8]

II. METHOD OF CALCULATIONS

In the atomic-sphere approximation the SSDW in the crystal can be described by the following spin-density distribution $\mathbf{m}(\mathbf{r})$:

$$\mathbf{m}(\mathbf{r})=\sum_i \eta(|\mathbf{r}-\mathbf{r}_i|)|\mathbf{m}(|\mathbf{r}-\mathbf{r}_i|)|\mathbf{e}_i\ ,$$
$$\mathbf{e}_i=(\sin\theta\cos(\mathbf{q}\cdot\mathbf{r}_i),\ \sin\theta\sin(\mathbf{q}\cdot\mathbf{r}_i),\ \cos\theta)\ , \tag{1}$$

where $\mathbf{r}_i$ is the radius vector of the ith atom and $\eta(|\mathbf{r}-\mathbf{r}_i|)$ is the function equal to 1 within the atomic sphere and zero outside the sphere. θ is the angle between the atomic moment and the global z axis, $\mathbf{e}_i$ is the unit vector in the direction of ith atom magnetic moment, and $\mathbf{q}$ is the spin-spiral vector, which defines the angle between the magnetic moments of neighboring layers. The arrangement of magnetic moments for some particular $\mathbf{q}$ value is given in Fig. 1 as an example. Being applied to the band-structure calculations, the distribution (1) leads to two problems: (a) the loss of translational symmetry of the crystal; and (b) the SSDW state is the excited state and the usual density-functional (DF) approach, which has been constructed for the ground state of the system of interacting electrons, is not directly applicable here. We have overcome these problems in the following way.

A. Multiple scattering in the crystal with SSDW

The first of the problems mentioned above can be solved in the scope of multiple scattering theory.[9,10] Single-site scattering is determined by the scattering t^{-1} matrix, which in the SSDW case is not diagonal in spin indexes. However, the $t_i^{-1}(E)$ matrix block correspond-

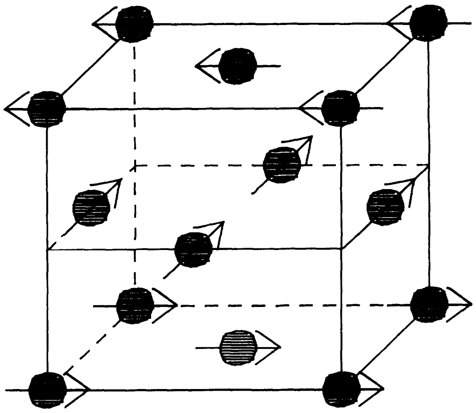

FIG. 1. Schematic picture of SSDW with $\mathbf{q}=q(0,0,1)$, $q=0.5$ (q is in units of $2\pi/a$), and $\theta=\pi/2$ in fcc lattice.

ing to the *i*th atom is diagonal in the local coordinate system (LCS), where the spin quantization axis is parallel to the atomic moment of the *i*th atom. In the global coordinate system (GCS) of the whole crystal the $\tilde{t}^{-1}$ matrix for the crystal with SSDW (1) can be defined by the relation

$$\tilde{t}^{-1}=Ut^{-1}U^{-1}\ , \tag{2}$$

where the U matrix is constructed from the spin-$\frac{1}{2}$ rotation matrices U_i connected with the *i*th atom. For the spin-density distribution (1) U_i is given by the relation

$$U_i(\theta,\mathbf{q})=\begin{bmatrix}\cos(\theta/2)\exp(i\mathbf{q}\cdot\mathbf{r}_i/2) & \sin(\theta/2)\exp(-i\mathbf{q}\cdot\mathbf{r}_i/2)\\ -\sin(\theta/2)\exp(i\mathbf{q}\cdot\mathbf{r}_i/2) & \cos(\theta/2)\exp(-i\mathbf{q}\cdot\mathbf{r}_i/2)\end{bmatrix} \tag{3}$$

and transforms the t_i^{-1} block from the LCS to the GCS for the *i*th atom. Then the energy spectrum of the crystal is defined by the usual secular equation:

$$\det\|g^{-1}\|=\det\|t^{-1}-S\|=0\ , \tag{4}$$

where the structure constants S depend on the crystal structure only. g is the scattering path operator. Using Eq. (2), the secular equation (4) for crystals with SSDW can be rewritten as follows:

$$\det\|\tilde{g}^{-1}\|=\det\|Ut^{-1}U-S\|=\det\|t^{-1}-\tilde{S}\|=0\ ,\qquad \tilde{S}=U^{-1}SU\ . \tag{5}$$

In the Bloch representation $\tilde{g}^{-1}$ has the form

$$\tilde{g}^{-1}_{L\alpha,L'\beta}(\mathbf{k},\mathbf{k}')=[t^{-1}_{L\alpha}(E)\delta_{LL'}\delta_{\alpha\beta}-\tilde{S}_{L\alpha,L'\beta}]\delta(\mathbf{k}-\mathbf{k}')\ . \tag{6}$$

Here L,L' are orbital and σ,σ' spin indexes. The $\tilde{g}^{-1}$ matrix appears to be diagonal over the wave-vector index.[6] This rather nontrivial result is a consequence of the generalized symmetry of the system and has been discussed by Sandratski.[11] We have obtained similar results in the scope of multiple scattering theory. The difference from Ref. 11, where general symmetry transformations of local magnetic moments in a crystal with spiral magnetic structure have been used, is that in the present paper we have considered the model of spiral-spin-density waves described by the spin-density distribution as defined by Eq. (1).

B. Density-functional formalism for longitudinal and transversal magnetic fluctuations

In the scope of the atomic-sphere approximation (ASA) model the spiral-spin-density wave defined by the distribution (1) can be described as the ground state of the system with the modified total energy functional:[12,6]

$$E^*[n,\mathbf{m}]=E[n,\mathbf{m}]+\sum_i\int_{v_i}d\mathbf{r}\{\mathbf{h}(\mathbf{r})[\mathbf{m}(\mathbf{r})-\mathbf{e}|\mathbf{m}(\mathbf{r})|]\}\ . \tag{7}$$

Here n and $\mathbf{m}$ are electron and spin densities and $\mathbf{h}(\mathbf{r})$ is the Lagrange parameter, which has the meaning of the field responsible for the fulfillment of the constraining condition (1). v_i is the volume of the *i*th atomic sphere. Longitudinal magnetic fluctuations may be considered in a similar way making use of the following energy functional:

$$E^*[n,\mathbf{m}]=E[n,\mathbf{m}]-\sum_i\mathbf{H}\left[\int_{v_i}d\mathbf{r}\,[\mathbf{m}(\mathbf{r})-\mathbf{m}_i]\right]\ , \tag{8}$$

obtained in accordance with the condition of certain magnitude of local moment $\mathbf{m}_i$ in the *i*th sphere:

$$\int_{v_i}d\mathbf{r}\,\mathbf{m}(\mathbf{r})=\mathbf{m}_i\ . \tag{9}$$

C. Estimations of magnetic interaction parameters

The LMTO band-structure calculations for the system with spiral-spin-density waves can be readily used for the estimation of exchange integrals in the Heisenberg model:

$$H_{\text{eff}}=-\sum_{i,j}J_{ij}\mathbf{S}_i\cdot\mathbf{S}_j\ . \tag{10}$$

The relevant expressions for exchange integrals J in the ferromagnetic case are as follows:[7,8]

$$J_{ij}=(1/4\pi)\sum_{i,j}\text{Im}\int_{\infty}^{E_F}d\varepsilon\,\Delta^i_l(\varepsilon)T^{ij\uparrow}_{LL'}(\varepsilon)\Delta^j_{l'}(\varepsilon)T^{ij\downarrow}_{LL'}(\varepsilon)\ , \tag{11}$$

$$\begin{aligned}J_{00}=-(1/4\pi)\int_{\infty}^{E_F}d\varepsilon\{&\Delta^0_l(\varepsilon)[T^{00\uparrow}_{LL'}(\varepsilon)-T^{00\downarrow}_{LL'}(\varepsilon)]\\&+\Delta^0_l(\varepsilon)T^{00\uparrow}_{LL'}(\varepsilon)\Delta^0_{l'}(\varepsilon)T^{00\downarrow}_{LL'}(\varepsilon)\}\ ,\end{aligned} \tag{12}$$

$$J_{00}=\sum_i J_{0i}\ . \tag{13}$$

Here $\mathbf{S}_i$ is the unit vector, which defines the direction of *i*th magnetic moment. $\Delta^i_l(\varepsilon)=P^i_{l\uparrow}(\varepsilon)-P^i_{l\downarrow}(\varepsilon)$, where $P^i_{l\sigma}(\varepsilon)$ are potential parameters of the LMTO method. $T^{ij\sigma}_{LL'}$ is the scattering path operator in the LMTO representation.

D. SSDW in the LMTO representation: computational details

In the scope of the LMTO approach[13] the secular equation (5) can be rewritten in the form

$$\det\|E-\tilde{H}\|=0 \tag{14}$$

with the Hamiltonian $\tilde{H}$:

$$\tilde{H}_{L\sigma L'\sigma'}(\mathbf{k})=V_{L\sigma}\delta_{LL'}\delta_{\sigma\sigma'}+\Gamma^{1/2}_{L\sigma}[Q-\tilde{S}(\mathbf{k})]^{-1}_{L\sigma L'\sigma'}\Gamma^{1/2}_{L'\sigma'}\ . \tag{15}$$

$\tilde{S}$ are the structure constants of the LMTO-SS method:[6]

$$\tilde{S}_{L\sigma L'\sigma'}(\mathbf{k})=S_{LL'}(\mathbf{k}-\mathbf{q}/2)\begin{bmatrix}\cos^2(\theta/2) & -\frac{1}{2}\sin\theta \\ -\frac{1}{2}\sin\theta & \sin^2(\theta/2)\end{bmatrix} + S_{LL'}(\mathbf{k}+\mathbf{q}/2)\begin{bmatrix}\sin^2(\theta/2) & \frac{1}{2}\sin\theta \\ \frac{1}{2}\sin\theta & \cos^2(\theta/2)\end{bmatrix} . \tag{16}$$

Here $S_{LL'}(\mathbf{k})$ are the structure constants of the usual LMTO method, and Γ, Q, and V are the potential parameters.[13] Recently similar expressions for $\tilde{S}$ have been obtained in the scope of the augmented-spherical-waves (ASW) method.[14] The other details of the self-consistent LMTO-SS method, which we used in the present calculations, are described in detail elsewhere.[6]

As is seen from Eqs. (15) and (16), the formation of spiral-spin-density wave leads to the shift of spin-up states by the SSDW vector $\mathbf{q}$, relative to the spin-down states, and to their hybridization. Thus, using the LMTO-SS Hamiltonian (15) and Eqs. (7) and (8) for the modified total energy functional, one can carry out the self-consistent calculations of the total energy for the particular spin-density wave state. In the present paper, we have carried out such calculations for Fe, Co, and Mn making use of the von Barth–Hedin exchange-correlation potential.[15]

III. RESULTS AND DISCUSSION

The total energies $E(q)$ and local magnetic moments $m(q)$ as functions of the modulus of spin-spiral vector $\mathbf{q}$ calculated for a γ-Fe crystal with different lattice parameters (the Wigner-Seitz radii S) are given in Figs. 2–4. For $S=2.66$, 2.69, and 2.72, the minimum of total energy corresponds to the SSDW state with $\mathbf{q}=0.6(0,0,1)$ (Figs. 2 and 3). Figure 3 shows also the total energy of SSDW with the other $\mathbf{q}$ vector: $\mathbf{q}=q(1,1,1)$. As is seen from the comparison of Figs. 2(a) and 4, the decrease of local magnetic moments for $S=2.69$ and 2.72 a.u. results in the decrease of the total energy. Such a behavior cannot be explained by a simple Stoner-like theory. The $m(q)$ dependence for $S=2.66$ a.u. differs greatly from the one found for the other atomic volumes. Two magnetic states exist for ferromagnetic (FM) ($q=0$) fcc iron, but only one for antiferromagnetic (AFM) ($q=1$) configuration. For all S values, except for $S=2.66$, the variation of q from 0 to 1 results in continuous transformation of the high-spin state for FM fcc iron into the most stable AFM state. At the same time, for $S=2.66$ the spiral states with $0\leq q\leq 0.5$ correspond obviously (Fig. 4) to the low-spin state of FM iron. For $q>0.5$ the nature of the states with the minimal total energy changes, and they are counted now with the only magnetic state of AFM fcc iron.

As is seen from Figs. 2 and 3 the most stable magnetic configuration of fcc iron at the crystal volumes, corresponding to $S=2.66$, 2.69, and 2.72 a.u., is the spiral-spin-density-wave state, which is consistent with the data.[4] Figure 2(b) shows that the decrease of crystal volume results in the decrease of the SSDW energy. But with the increase of S value, the tendency to the formation of a FM high-spin state becomes more pronounced and for $S=2.78$ a.u. fcc iron is already ferromagnetic (as is true for fcc Fe precipitates in Cu-Au alloys[1]).

The dependence of $E(q)$ minimum on the number of valence electrons becomes obvious from Fig. 5, where the results of similar calculations for fcc Co and Mn are presented (obtained with the same Wigner-Seitz radius value $S=2.69$). An increase in the number of valence electrons leads to the stabilization of ferromagnetic ordering (fcc Co), but a decrease tends to stabilize the antiferromagnetic configuration (fcc Mn). Thus our results show that for a fcc lattice Fe is located at the crossing point between the ferromagnetic and antiferromagnetic ordering and exists in the spiral-spin-density-wave state.

The exchange parameters estimated for fcc and bcc iron making use of Eqs. (11) and (12) are given in Table I. The J_{0i} values for five shells of the nearest neighbors together with the spin wave stiffness constants are presented.

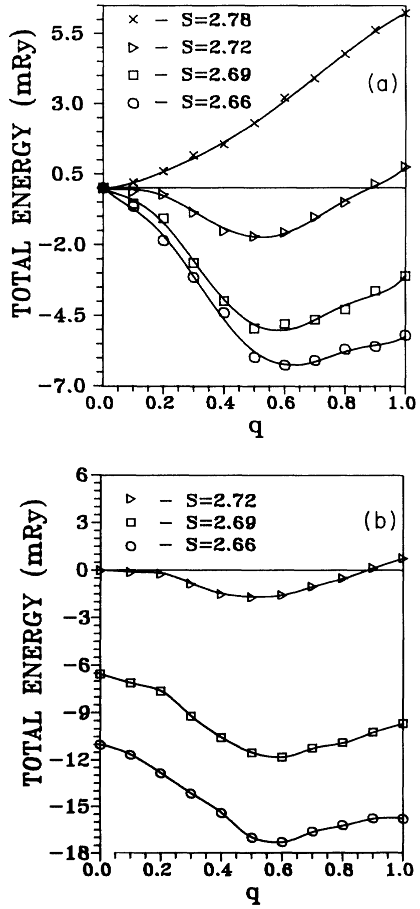

FIG. 2. The total energy of spiral-spin-density-wave states with $\mathbf{q}=q(0,0,1)$ for fcc Fe: (a) relative to that of ferromagnetic state of the crystal with the same S; (b) relative to the total energy of ferromagnetic crystal with $S=2.72$ a.u. S is the Wigner-Seitz radius for fcc lattice.

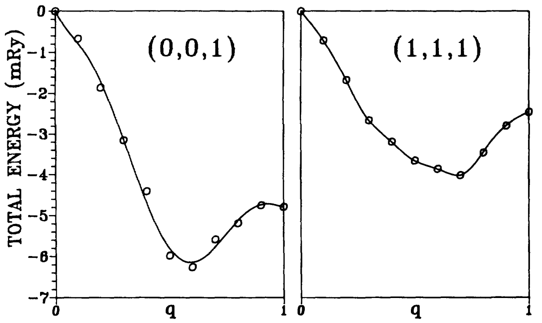

FIG. 3. The total energy of SSDW $\mathbf{q}=q(0,0,1)$ and $q(1,1,1)$ relative to that of ferromagnetic fcc Fe. $S=2.66$ a.u. q is in $q_{\max}$ units, $q_{\max}$ is the maximum absolute value of $\mathbf{q}$ relative to that of ferromagnetic fcc Fe. $S=2.66$ a.u.

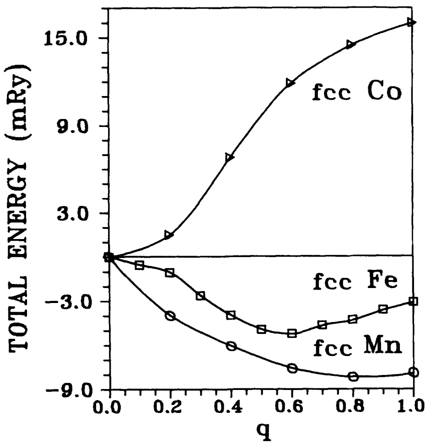

FIG. 5. The total energy of the SSDW states for fcc Co, Fe, and Mn.

The magnitude of spin-stiffness constant for bcc iron calculated with the use of effective exchange integrals given in Table I (Ref. 8) agrees rather well with the experimental data available. As is seen, ferromagnetic interactions prevail in bcc iron. The magnetic behavior of fcc iron has a more complicated and long-range nature (see Table I). In this case, effective exchange interaction parameter J_{01} for the first coordination sphere is negative, but J_{02} for the second sphere is positive. Such a behavior of exchange interaction is one of the possible reasons for the formation of noncollinear magnetic structure.[16] However, for the itinerant magnetics a strong dependence of exchange interactions on the particular magnetic configuration is possible.[17,18] The J_{0i} values in Table I have been obtained for the ferromagnetic fcc iron.[7] Nevertheless, the decrease of the total energy for the low q values (Fig. 2) can be explained by the J_{01} and J_{02} values obtained in the scope of a simple Heisenberg model. At the same time the description of total energy minimum at $q=0.6$ in the scope of such a simple model requires the account of more distant interactions.[8] In other words, the appearance of total energy minimum at $q=0.6$ can be attributed to some definite electronic states, which are rather localized in the k space. We have made their analysis using the results of our calculations.

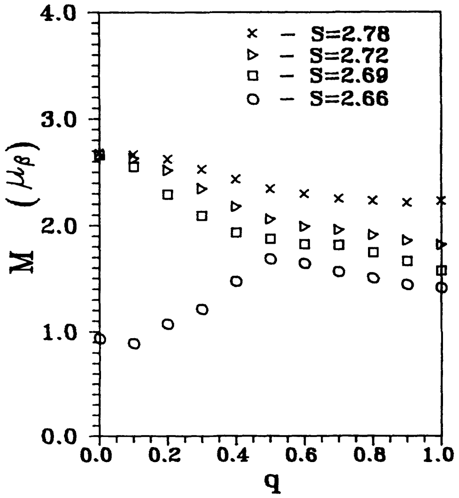

FIG. 4. Local magnetic moment in fcc Fe as a function of spin-spiral vector $\mathbf{q}$.

The band structure of nonmagnetic fcc iron ($S=2.66$ a.u.), as calculated by the non-self-consistent LMTO-SS method [with the spin-up states shifted relative to the spin-down states by the vector $q=0.6(0,0,1)$] is presented in Fig. 6(a). Figure 6(b) shows the self-consistent bands for the SSDW state. As is seen from their comparison, the influence of exchange interactions (exchange splitting and hybridization of up and down states) is the most prominent near the Γ and X points. The detailed structure of the states near the Fermi level for the Γ-X direction is shown in Figs. 7(a) and 7(c), correspondingly. The band structure of ferromagnetic fcc Fe ($S=2.66$) with the $\sigma=\pm1$ states shifted by $\pm\mathbf{q}/2$, $\mathbf{q}=0.6(0,0,1)$ is shown in Fig. 7(b).

When the atomic volume changes, three mechanisms appear to be responsible for total energy changes. They are as follows: (1) the shift of spin-up and spin-down states relative to each other; (2) exchange splitting of these states; and (3) hybridization of $\sigma=\pm1$ states. All of them are illustrated in Fig. 7: Fig. 7(a) represents the first mechanism, Fig. 7(b) corresponds to the second and first mechanisms together, Fig. 7(c) shows the final result when all three mechanisms are in effect.

The variation of crystal volume leads to the changes of relevant contributions of different mechanisms. For $S=2.66$ all three mechanisms are comparable and important. For $S=2.69$ and 2.72 the third mechanism is much less important as compared with the second and first ones (due to the large spin splitting). In this case the Heisenberg model is a rather good approximation and the total energy of SSDW relative to that of the ferromagnetic state can be written as follows:

$$\Delta E(\mathbf{q})=J(0)-J(\mathbf{q}) , \tag{17}$$

$$J(\mathbf{q})=\sum_i J_{0i}\exp(i\mathbf{q}\cdot\mathbf{r}_i) . \tag{18}$$

TABLE I. Effective parameters of exchange interactions J_{0i} in Fe (mRy) and spin wave stiffness constant D^{theor} (meV Å^2). The experimental value D^{exp} is 330 (meV Å^2).

Crystal structure	J_{01}	J_{02}	J_{03}	J_{04}	J_{05}	J_{00}	D^{theor}
bcc, $S=2.66$	1.00	0.60	-0.02			10.69	300
fcc, $S=2.66$	-0.19	0.13	-0.03	0.10	-0.04	-2.29	
fcc, $S=2.69$	0.09	0.027	-0.29	0.59	-0.06	-0.80	
fcc, $S=2.72$	0.48	0.41	-0.27	0.41	-0.02	5.05	
fcc, $S=2.78$	0.82	0.39	-0.23	0.30	-0.02	9.21	

Here J_{0i} is the exchange interaction parameter, which may be calculated for the ferromagnetic state.[7,8] Thus for the high-spin state ($S=2.69$) the model of localized magnetic moments reasonably describes the dependence $E(\mathbf{q})$. In the low-spin case ($S=2.66$) the itinerant magnetism is revealed and leads to the strong $J(\mathbf{q})$ dependence.[19]

The decrease of the crystal volume ($S \leq 2.66$) results in the decrease of the third and second mechanism contributions, as compared with the first one because of the essential decrease of spin splitting. In the case ($m \ll 1$) total energy differences may be written as follows:

$$\Delta E(\mathbf{q})=I^2[\chi(0)-\chi(\mathbf{q})] \ . \tag{19}$$

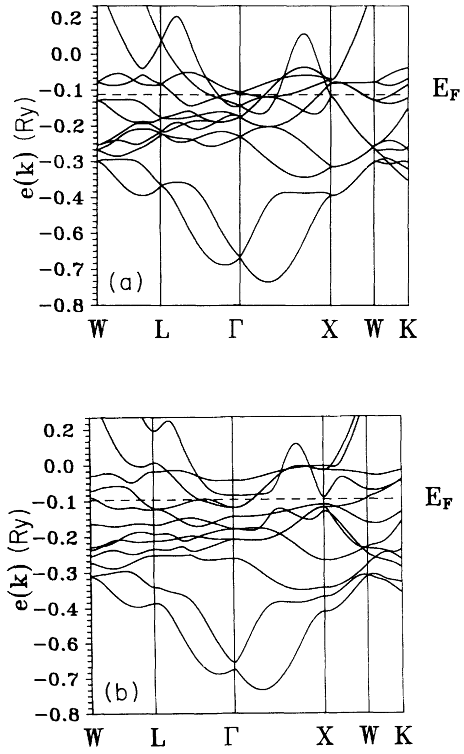

FIG. 6. Band structure of fcc Fe as calculated by the LMTO-SS method: (a) non-self-consistent calculation of nonmagnetic fcc iron; bands with $\sigma=\pm1$ are shifted by $\pm\mathbf{q}/2$, $\mathbf{q}=0.6(0,0,1)$. The Wigner-Seitz radius $S=2.66$ a.u. (b) Same as for (a), but corresponding to the self-consistent SSDW calculation with the same $\mathbf{q}$ vector.

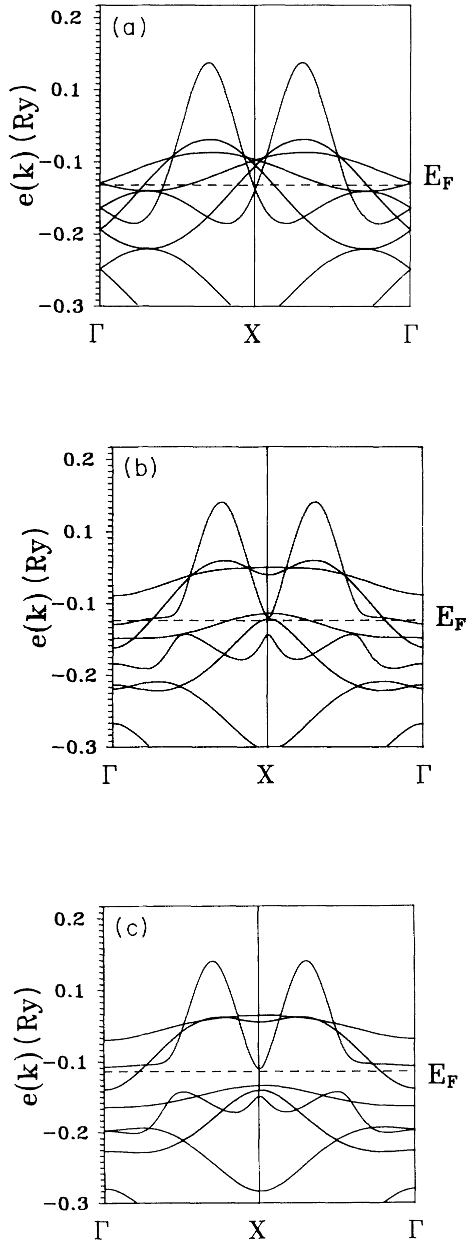

FIG. 7. Energy bands for fcc iron near the Fermi level: (a) Nonmagnetic crystal. The bands with $\sigma=\pm1$ are shifted as in Fig. 6(a). (b) Ferromagnetic fcc iron with the states $\sigma=\pm1$ shifted by $q=0.6(0,0,1)$. (c) Spiral-spin-density state of fcc Fe with SSDW $\mathbf{q}=0.6(0,0,1)$ (self-consistent calculation).

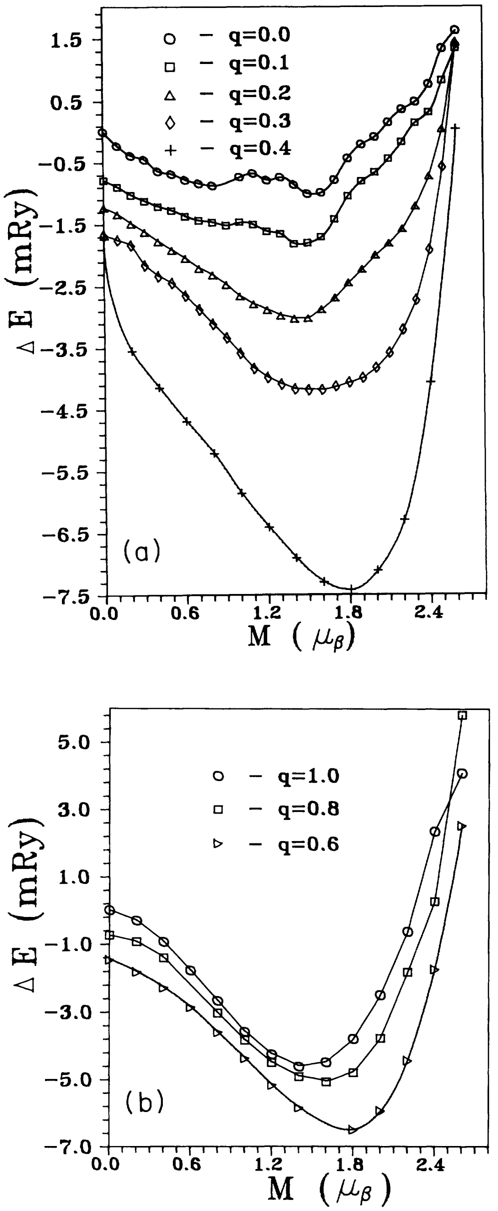

FIG. 8. Total energy of fcc Fe ($S=2.66$ a.u.) as a function of magnetic moment M and SSDW vector $\mathbf{q}=q(0,0,1)$ as compared with that of nonmagnetic state calculated by the LMTO-SS method for the same q: (a) Ferromagneticlike SSDW states with $q=0,0.1,0.2,0.3,0.4$; zero point is the total energy of nonmagnetic state with $q=0$. (b) Antiferromagneticlike SSDW states with $q=1.0,0.8,0.6$. Zero point is the total energy of nonmagnetic state with $q=1$.

Here I is the effective intra-atomic Coulomb integral and $\chi(q)$ is an unenhanced spin susceptibility. Thus, as is seen, any conclusions based on the calculations of unenhanced spin susceptibility[5] are accurate only for small crystal volumes. As has been shown in Ref. 5, the susceptibility has the maximum at $q=(1,\frac{7}{48},0)$, which is in agreement with the neutron experiment results.[4] But the ASW calculations[14] give an idea of the shallow total energy minimum at $\mathbf{q}=(1,0.3,0)$. However, two of these possible states $\mathbf{q}=0.6(0,0,1)$ and $\mathbf{q}=(1,0.3,0)$ are so close in energy that they cannot be resolved basing on the ASW calculations. It is worth noting that the experimentally found magnetic state [SSDW with $\mathbf{q}=(1,0.123,0)$] apparently has rather small magnetic moment[2] and the SSDW state is defined by the peculiarities of the electronic structure of the nonmagnetic state. As is known, the Invar properties of γ-Fe-based alloys can be connected with rather complicated dependence of the total energy on the value and directions of magnetic moments in γ-Fe.[20] The dependence of the total energy changes (relative to that of the nonmagnetic state) on the local magnetic moment value for the different spin-density waves (ferromagneticlike for $q=0.0,0.1,0.2,0.3,0.4$ and antiferromagneticlike for $q=1.0,0.8,0.6$) is given in Fig. 8. As is obvious, even for the SSDW with small q values the local minima corresponding to the different magnetic states at $q=0$ disappear. We have performed the self-consistent total energy calculations for fcc iron taking into account the possibilities of both transversal (q dependent) and longitudinal (M dependent) fluctuations of spin density. Such calculations imply minimization of the modified total energy functional (7) and (8) with an additional (other than the electroneutrality of the unit cell) condition for fixed magnetic moment in the atomic sphere. The fixed magnetic moment procedure used was similar to that for collinear magnetics.[20] The magnetic field $\mathbf{H}$ in the modified functional (8) was calculated in the self-consistent way. Figures 8(a) and 8(b) show the total energies relative to those of the nonmagnetic state for the same q value. The differences in total energy for nonmagnetic fcc Fe calculated for different q are due to zero net moment, but nonzero spin density. The shift of degenerate in nonmagnetic state bands for the different q values may lead to some different accuracies in the band structure and spin-density calculations. The global total energy minimum is located near the point $(\mathbf{q}=0.6(0,0,1),M=1.8)$. Taking that into consideration, the Invar properties of γ-Fe-Ni alloys can be more reasonably explained making use of the suggestion on the antiferromagnetic nature of γ-Fe,[21] but in order to make such an explanation more reliable noncollinear antiferromagnetism of γ-Fe should be considered.

The results obtained are promising and show that quantitative band-structure calculations of noncollinear magnetic systems may well be in the scope of the approaches similar to the one developed in the present paper.

ACKNOWLEDGMENT

One of us (V.A.G.) is grateful to Professor A. J. Freeman for stimulating discussions and hospitality during his stay at Northwestern University.

[1] U. Gonser, K. Krische, and S. Nasu, J. Magn. Magn. Mater. **15-18**, 1145 (1980).

[2] Y. Tsunoda, J. Phys. Condens. Matter **1**, 10 427 (1988).

[3] V. L. Moruzzi, P. M. Marcus, K. Schwarz, and P. Mohn, Phys. Rev. B. **34**, 1784 (1986).

[4] L. S. Wang, B. M. Klein, and H. Krakauer, Phys. Rev. Lett. **54**, 1852 (1985).

[5] K. Hirai, J. Phys. Soc. Jpn. **58**, 4288 (1989).

[6] O. N. Mryasov, A. I. Liechtenstein, L. M. Sandratski, and V. A. Gubanov, J. Phys. C **3**, 7683 (1991).

[7] A. I. Liechtenstein, M. I. Katznelson, and V. A. Gubanov, J. Phys. F **14**, L125 (1984).

[8] A. I. Liechtenstein, O. N. Mryasov, L. M. Sandratski, and V. A. Gubanov (unpublished).

[9] P. Lloyd and P. V. Smith, Adv. Phys. **21**, 69 (1972).

[10] B. L. Gyorfy and G. M. Stocks, in *Electrons in Disordered Metals and Metallic Surfaces,* edited by P. Phariqeau, B. L. Görffy, and L. Scheire (Plenum, New York, 1979), p. 89.

[11] L. M. Sandratski, Phys. Status Solidi B **135**, 167 (1986).

[12] P. H. Dederichs, S. Blugel, R. Zeller, and H. Akai, Phys. Rev. Lett. **53**, 2512 (1984).

[13] O. Gunnarson, J. Jepsen, and O. K. Andersen, Phys. Rev. B **27**, 7144 (1983).

[14] M. Uhl, L. M. Sandratski, and J. Kubler, J. Magn. Magn. Mater. **103**, 314 (1992).

[15] U. von Barth and L. Hedin, J. Phys. C **5**, 1629 (1972).

[16] A. Yoshimori, J. Phys. Soc. Jpn. **14**, 807 (1959).

[17] M. U. Luchini and V. Heine, Europhys. Lett. **14**, 609 (1991).

[18] V. Heine, A. I. Liechtenstein, and O. N. Mryasov, Europhys. Lett. **12**, 545 (1990).

[19] H. Hasegawa, Physica B **119**, 15 (1983).

[20] K. Schwarz and P. Mohn, J. Phys. F **14**, L129 (1984).

[21] E. N. Kondorsky, and V. L. Sedov, Zh. Eksp. Teor. Fiz. **38**, 773 (1960) [Sov. Phys. JETP **11**, 561 (1960)].